Dynamics of inherent structure in supercooled liquids near kinetic glass transition

C. Y. Liao and S.-H. Chen
Department of Nuclear Engineering, Massachusetts Institute of Technology, Cambridge, Massachusetts 02139
(Received 12 August 2000; published 27 August 2001)

We present a description of the dynamics of a supercooled binary Lennard-Jones liquid in term of the potential landscape of the system. The slowing down of the dynamics in supercooled liquids near the kinetic glass transition is related to the existence of basins in the potential landscape. The inherent structures that are the local potential minima in the configuration space obtained by a quench process are employed to represent the configurations of the basins. We present time correlation functions of the inherent structure, both the self and the coherent part, as a function of wave vector. We also calculated the mean-square displacement, and the non-Gaussian parameter of the van Hove self-correlation function. Compared with the dynamics of original configurations, the short-time relaxation has almost been eliminated by the quench process. However, the long-time α relaxations remain essentially the same. We conclude that the long-time α relaxation is the result of cross-basin transition in the potential landscape in the configuration space.

DOI: 10.1103/PhysRevE.64.031202 PACS number(s): 61.20.Ja, 64.70.Pf

I. INTRODUCTION

It is well known that the relaxation dynamics of the supercooled liquids near kinetic glass transition is a two-step process. This characteristic feature has been shown by the mode-coupling theory [1,2], computer molecular-dynamics simulation [3], and laboratory experiments involving glass-forming liquids(for review see [4]). From the kinetic theoretic point of view, the short-time dynamics within a picosecond time scale is describable by the relaxation of the test particle motion within a cage formed by nearest-neighboring particles in the liquid, which can be described by a normal kinetic theory of liquid, taking into account the cage effect [5]. The long-time dynamics (α relaxation) is pictured as the collective relaxation of the initial cage and is insensitive to the specific short-time microscopic dynamics of the system within the cage [6].

The potential landscape view of the dynamics of supercooled liquids near kinetic glass transition was presented a long time ago [7,8]. But recently it has attracted much attentions both from the dynamic and thermodynamic approaches [9–11]. According to these views, the slowing down of the long-time relaxation process was related to the presence of the potential basins in the configuration space and could be regarded as the configurational transitions between these basins. The short-time relaxation was regarded as the exploration of the phase points of the system within the same potential basin. The lowering of the temperature of the system does not affect the intrabasin movement too much, but will make the crossing between basins more difficult and time consuming. We comment here that in the kinetic theoretic picture, the long-time collective cage relaxation is not a local relaxation phenomenon, but should be considered globally as interbasin transitions in the potential landscape.

In order to study the long-time interbasin transitions in the potential landscape, one has to introduce the inherent structure, which is defined as the local potential minima in the configuration space, as the best configurational representation of the corresponding basin [12]. Then, by studying the changing of the inherent structure with time, one can eliminate most of the short-time relaxation process within the basin and only focus on the long time interbasin relaxation. The dynamics of inherent structure has been studied in different ways. The interbasin transition was identified by examining the level changes of the energy of inherent structure [13], the mean square displacement of the inherent structure was shown without a plateau because of the lack of constrained motions (rattling) within basins [14]. More recently, Schroder *et al.* [15] studied the self-time correlation functions of the quenched configurations at one value of k and at different temperatures and got the conclusion that the long-time relaxation is due to the interbasin transitions in the potential landscape. We know the interbasin transitions are the collective motions of particles in the system. In order to have a clearer picture of the interbasin transitions, one has to investigate the collective motions by calculating the coherent correlation functions of inherent structure in different length scales.

In this paper, we present the time correlation functions of the inherent structure, both the self and coherent part, at different k values. The two-step relaxations with a plateau in between, shown in the time correlation function of the original configurations, change to one-step relaxations without a plateau. This one-step decay curve can be characterized by a stretched exponential function having the same relaxation time τ and similar stretch exponent β with the α relaxation of the original configurations. This is a direct evidence from the coherent correlation function that the α relaxation in the supercooled liquids is due to the relaxation of cross-basin processes.

II. NUMERICAL SIMULATION

The model system for glass-forming liquids we studied is the well-known binary Lennard-Jones mixture introduced by Kob and Andersen [16,17]. Both types of classical particles A and B have the same mass and interact by a Lennard-Jones potential, i.e., $V_{\alpha\beta}(r)=4\epsilon_{\alpha\beta}[(\sigma_{\alpha\beta}/r)^{12}-(\sigma_{\alpha\beta}/r)^{6}]$ with $\alpha,\beta\in\{A,B\}$ and $\epsilon_{AA}=1.0$, $\sigma_{AA}=1.0$, $\epsilon_{AB}=1.5$, $\sigma_{AB}=0.8$, $\epsilon_{BB}=0.5$, $\sigma_{BB}=0.88$. In the following, all the results will be given in reduced units, i.e., length in units of σ_{AA}, energy in units of ϵ_{AA}, mass in units of the mass of particle A or B, which has been chosen as 1, and time in units of

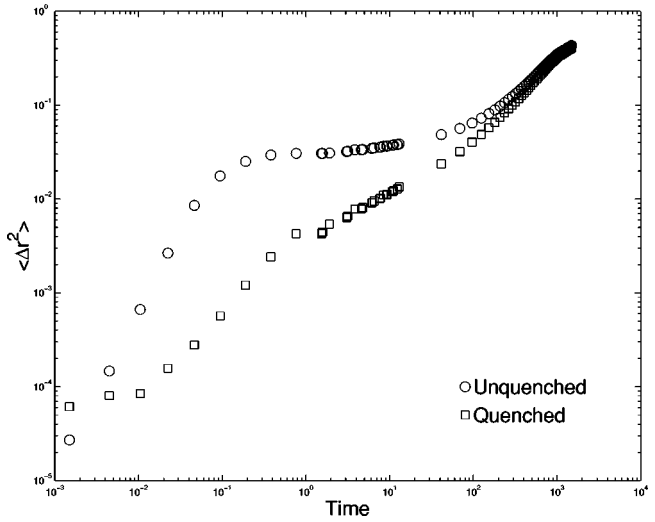

FIG. 1. The mean-square displacements (MSD) as a function of elapsed time for both unquenched and quenched configurations. The plateau that indicates the cage effects in the unquenched MSD disappears in the quenched MSD curves. They both show the same long-time diffusion limit.

$(m\sigma_{AA}^2/\epsilon_{AA})^{1/2}$. The Boltzmann constant k_B has been set to 1. The simulation box mixed 800 particles of type *A* and 200 particles of type *B*. The size of the cubic box was held fixed at $L=9.4$ with a periodic boundary condition. The critical temperature for a diverging relaxation time in this system is $T_c=0.435$. In our simulation, the simulation time-step size is 0.0015, the temperature is set at $T=0.446$, coupled with a Nose-Hoover thermostat [18].

We denote the molecular-dymamics (MD) trajectory as $[\mathbf{r}^N(t),\mathbf{p}^N(t)]$, with *N* the total number of particles. From each saved configuration $\mathbf{r}^N(t)$ at time *t*, the corresponding inherent structure $\mathbf{r}^{NQ}(t)$ was calculated as the local potential minima in the configuration space by the process of quench. The quench was accomplished by using a standard conjugate-gradient minimization algorithm [19]. We studied the two types of trajectories: unquenched and quenched trajectories, by comparing some meaningful dynamic quantities calculated from these two trajectories. The mean square displacement between these two configurations $\langle|\mathbf{r}_j(t)-\mathbf{r}_j^Q(t)|^2\rangle$ gives the mean value of 0.0142 with a standard deviation of 0.0015, which is related to the average size of trapping basin. The size of the trapping basin can also be characterized by the plateau value (about 0.03) of mean square displacement (MSD) of unquenched configurations discussed in the next paragraph. We can see these two values are of the similar magnitude.

The mean square displacements (MSD) $\langle\Delta r^2(t)\rangle=\langle|\mathbf{r}_j(t)-\mathbf{r}_j(0)|^2\rangle$ of the unquenched configuration as a function of elapsed time is shown in Fig. 1 in a log-log plot. The MSD of quenched configurations, shown in the same figure, is calculated by replacing the configuration $\mathbf{r}(t)$ in the formula of MSD by the quenched configuration $\mathbf{r}^Q(t)$. The existence of a plateau of the unquenched configuration shows the trapping effect of the system inside a basin in the potential landscape. For the quenched configuration, the MSD is a monotonic increasing function with time without a plateau. This is because the quench process eliminates the system vibrational movement inside the trapping basin. At a large elapsed time segment in the diffusion region $t>1000$, the MSD's of these two configurations overlap with each other showing the different motions between these two configurations, which are the small-distance vibrational movement within the basin, can be ignored compared with the structural relaxation as a result of large distance excursions.

We define the van Hove self-correlation function as [20]

$$G_s(\mathbf{r},t)=\frac{1}{N}\left\langle\sum_j \delta[\mathbf{r}+\mathbf{r}_j(0)-\mathbf{r}_j(t)]\right\rangle, \tag{1}$$

where the position of the jth particle $\mathbf{r}_j(t)$ can be a quenched or unquenched configuration. For the convenience in the following discussion without further explanation, the quantities calculated from quenched and original unquenched configurations will be denoted with and without label *Q*, respectively. For the isotropic system, the van Hove self-correlation function can be written as a function of radial distance *r* as $G_s(r,t)$. Then, the quantity $4\pi r^2G_s(r,t)$, integrated over the solid angle, denotes the distribution function of particle displacement *r* within time *t*. Compared with the distribution function of displacement of unquenched configurations, Fig. 2 shows that the quench process makes the distribution peak shift to the left and become sharper, indicating that the displacement of quenched configurations is much less than that of the original configurations. This can also be seen from the MSD curve (see Fig. 1), which is the second moment of the distribution function. In the intermediate times ($6<t<120$), the shape of $4\pi r^2G_s(r,t)$ changes much slower than that of $4\pi r^2G_s^Q(r,t)$. This slower variation of the curve shape with time causes the existence of the plateau in the MSD curve. In the long-time regime ($t>120$), the large displacements become more probable in both cases. At the largest time ($t=1350$), the two curves $[4\pi r^2G_s(r,t),4\pi r^2G_s^Q(r,t)]$ become essentially the same. This can also be seen from the similar value of the non-Gaussian parameter $\alpha_2(t)$ (Fig. 3) at that time. The non-Gaussian parameter is defined as [21,22]

$$\alpha_2(t)=\frac{3\langle r^4(t)\rangle}{5\langle r^2(t)\rangle^2}-1. \tag{2}$$

In the short-time free streaming and long-time diffusion limits, the van Hove self-correlation function is a Gaussian function with *r* [21], then the non-Gaussian parameter $\alpha_2(t)=0$. In the immediate time, the van Hove self-correlation function shows a clear non-Gaussian behavior. The non-Guassian parameter of quenched configurations have a large value in the short time and intermediate time; only in the long time do the values become similar as that of the unquenched configurations.

III. RESULTS

We calculated the coherent time correlation function of density fluctuation by

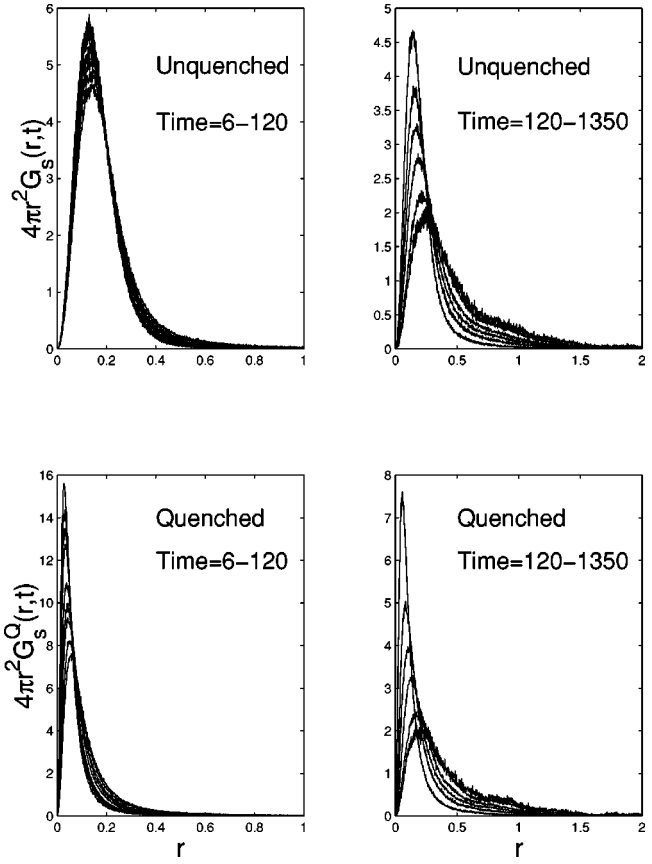

FIG. 2. The distribution function of the test particle displacements, $4\pi r^2 G_s(r,t)$, at different time segments. The van Hove self-correlation function is $G_s(\mathbf{r},t)=1/N\langle\Sigma_j \delta[\mathbf{r}+\mathbf{r}_j(0)-\mathbf{r}_j(t)]\rangle$. While at the intermediate time segment ($t=6$–120), the time variation of distribution functions of two configurations are quite different (see text), at the long-time segment ($t>120$), the time variations are similar in the two configurations.

$$F(k,t)=\frac{1}{N}\sum_{i,j}\langle\exp\{-\mathbf{k}\cdot[\mathbf{r}_i(t)-\mathbf{r}_j(0)]\}\rangle, \qquad (3)$$

where i, j denote the indices of the particles, and the configuration $\mathbf{r}^N(t)$ can be quenched or unquenched. The initial value of $F(k,t)$ is the static structure factor, $F(k,t=0)=S(k)$. Figure 4 shows the static structure factor $S(k)$ and $S^Q(k)$. The two curves display essentially the same first and second diffraction peaks, but a significant difference at larger k, where the quenched structure factor shows sharper peaks than the original one. The similarity of the first two peaks indicates that the two configurations are similar at the length scale $r>0.5\sigma_{AA}$, the quench process only changes the positions of the particles in the length scale of less than $0.5\sigma_{AA}$. This agrees with the MSD value between quenched and unquenched configurations discussed above. Since the structure factor is an average function of the configurations, the more smooth peaks at high-k value for the unquenched configurations indicate the more averaging effect due to the rattling movement around the quenched configurations with a rather small distance.

The normalized $F(k,t)/S(k)$ and $F^Q(k,t)/S^Q(k)$ are shown in Fig. 5 at $k\sigma_{AA}=6.68$. The $F(k,t)/S(k)$ shows a normal two-step decay, with a short-time decay first to a plateau characterized by a k-dependent Debye-Waller factor $A(k)$ and then an α relaxation away from the plateau. The appearance of the Debye-Waller factor is the result of the cage effect, which constrains the system into a basin area in the configuration space. On the contrary, The curve of $F^Q(k,t)/S^Q(k)$ shows a monotonic decay without a plateau. The short-time decay in the original correlation function is eliminated by the quench process. The decay of the quenched correlation function can be regarded as the system movement by crossing different basins in the configuration space.

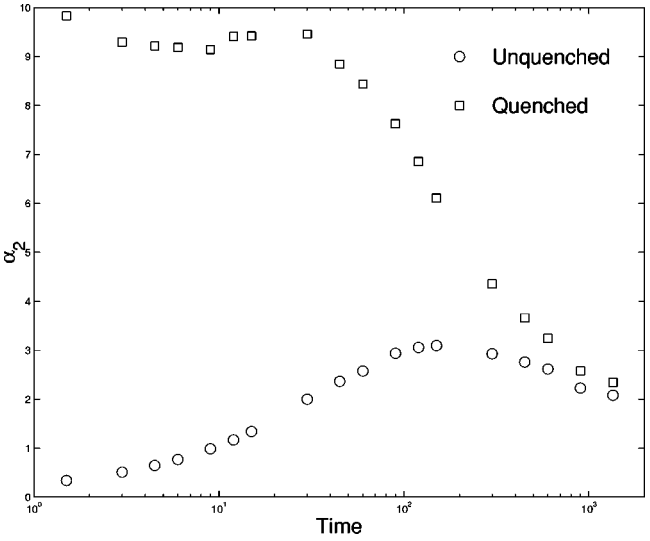

FIG. 3. The non-Gaussian parameters $\alpha_2(t)$ in the intermediate and long-time regime for the two types of configurations. While at the short-time regime, the non-Gaussian parameters of the two configurations are quite different, at the long-time regime they converge to the same asymptotic limit.

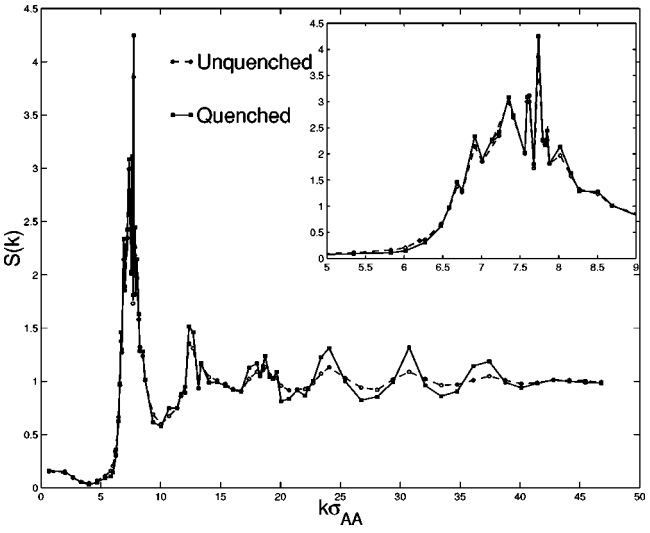

FIG. 4. The structure factor $S(k)$ and $S^Q(k)$, calculated from unquenched and quenched configurations. Note that the first two diffraction peaks are essentially the same. But at the large k values, the quenched $S^Q(k)$ displays sharper higher-order diffraction peaks. The inset shows the enlarged first diffraction peak region.

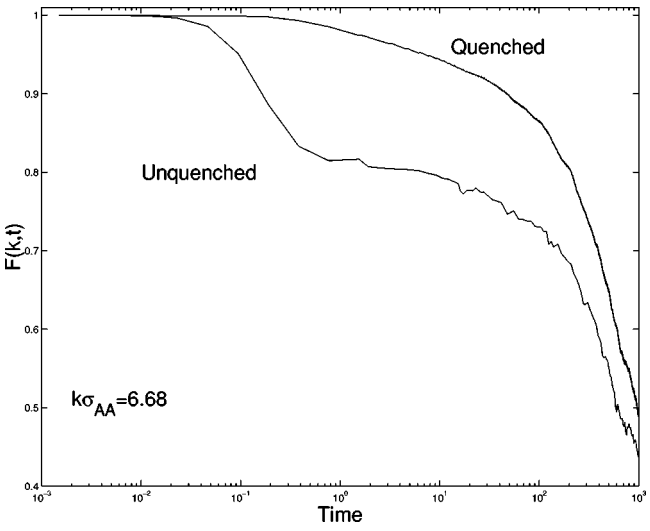

FIG. 5. The normalized coherent correlation function $F(k,t)/S(k)$ and $F^Q(k,t)/S^Q(k)$ at the reduced k value indicated. While the unquenched configurations show a two-step relaxation (fast and slow), the quenched configurations show only the slow relaxation.

To qualify and compare the long-time decay of $F(k,t)/S(k)$ and $F^Q(k,t)/S^Q(k)$, we fit the long-time part of the correlation function with the stretched exponential function $A(k)\exp(-(t/\tau(k))^{\beta(k)})$. Figure 6 shows that relaxation time τ, stretch exponent β, and Debye-Waller factor $A(k)$ oscillate with the same period as the structure factor. This agrees qualitatively with the result of extended simple point charge (SPC/E) water [23] and (MCT) theory [24]. Comparing the fitting results for $F(k,t)/S(k)$ and $F^Q(k,t)/S^Q(k)$, the relaxation times τ are essentially the same for all the k values, the exponent β demonstrates a similar variation with k but a level difference for $k\sigma_{AA}>10$. The Debye-Waller factor for the quenched system is much closer to unity than the unquenched system due to the elimination of the short-time dynamics. We note that the the k dependence of the Debye-Waller factor has been reduced and the oscillation has been damped compared with the unquenched system. But the k dependence of the relaxation time and stretch exponent in the quenched system is essentially the same as in the unquenched system. The difference between the quenched Debye-Waller factor and the unity indicates that the short-time dynamics is not eliminated completely or the basin roughness of the potential surface in the configuration space cannot be reduced by the quench process. This point will be discussed further.

The incoherent time correlation function studies the dynamics of a test particle, which is defined as

$$F_s(k,t)=\langle\exp[-\mathbf{k}\cdot\{\mathbf{r}_j(t)-\mathbf{r}_j(0)\}]\rangle, \tag{4}$$

where $\mathbf{r}_j(t)$ is the position of the jth particle, which can be a quenched or unquenched configuration. The initial value of $F_s(k,t=0)$ is one. Figure 7 shows the $F_s(k,t)$ and $F_s^Q(k,t)$ at different k values. $F_s(k,t)$ is found to display the typical two-step relaxation, where the short-time decay is attributed to the vibrational relaxation of particles with different frequencies within cages formed by neighboring particles

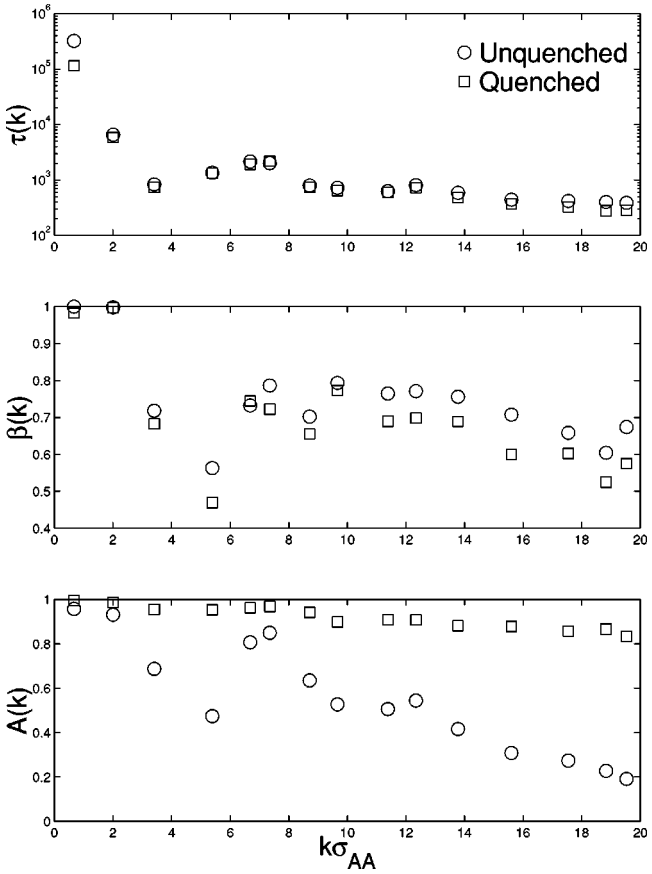

FIG. 6. The relaxation time $\tau(k)$, stretch exponent $\beta(k)$, and the Debye-Waller factor $A(k)$ extracted from the normalized coherent time correlation function, $F(k,t)/S(k)$ and $F^Q(k,t)/S^Q(k)$, by fitting the long-time part of the respective correlation functions with a stretched exponential function. While the τ and β are essentially the same for the two configurations, the Debye-Waller factors are significantly different. The quenched Debye-Waller factors are essentially unity at all k signifying that the system is not structurally arrested in the quenched configuration. It should be noted that there is k-dependent oscillation of all three parameters associated with variation of $S(k)$.

[25,26]. The long-time relaxation is separated from the short-time regime by a plateau indicating the trapping effect of cages. As expected, the plateau of $F_s^Q(k,t)$ disappears as the result of the quench process to remove the rattling movement that has been show in Ref. [15].

The quantitative comparison of the two incoherent time correlation functions can be studied by fitting the long-time part with the stretched exponential function $A(k)\exp\{-[t/\tau(k)]^{\beta(k)}\}$. Figure 8 shows the relaxation time $\tau(k)$, stretched exponent $\beta(k)$, and the Debye-Waller factor $A(k)$. The relaxation time is essentially the same for both quenched and original configurations. The $\beta(k)$ increase to the unity reaching diffusion regime as k decreases. The small difference of the β values of two configurations and the fact that the Debye-Waller factor of the quenched configurations is less than one indicates that, in the temperature investigated, the long-time dynamics cannot be separated completely from the short-time dynamics. This is a similar effect as in the coherent correlation function, which means there is

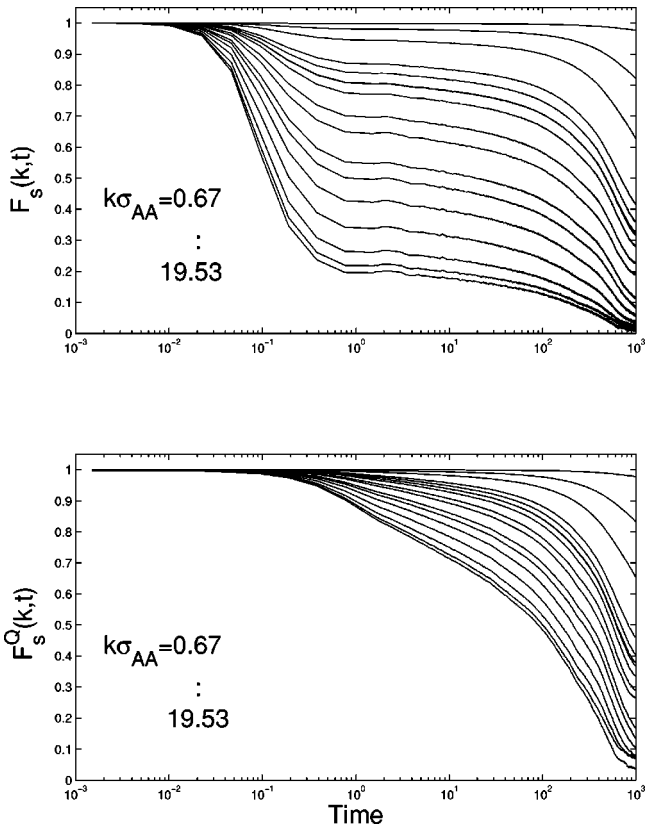

FIG. 7. The incoherent correlation function $F_s(k,t)$ (top) and $F_s^Q(k,t)$ (bottom), calculated from unquenched and quenched configurations at different k values from $k\sigma_{AA}=0.67$ to 19.53 (from the upper curve to the lower ones).

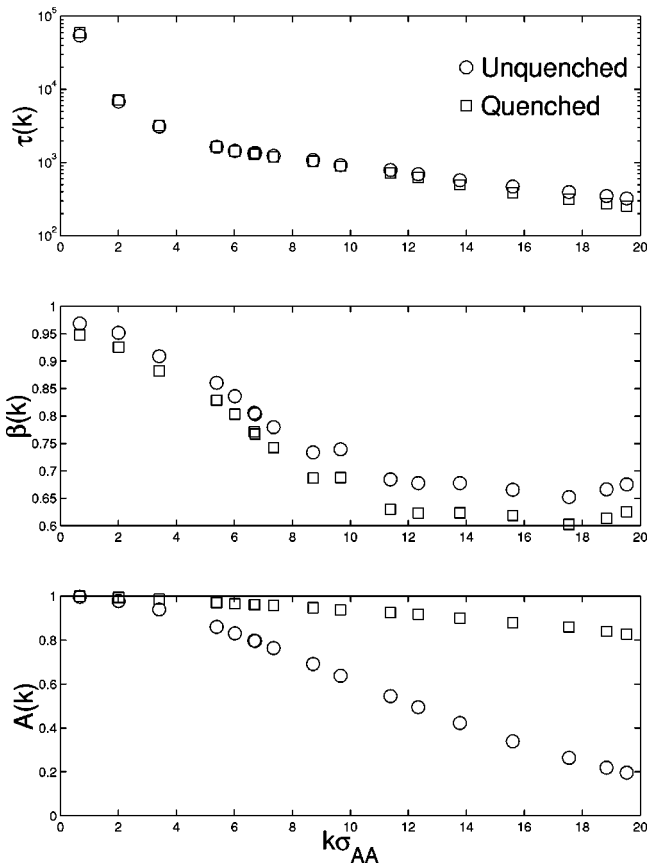

FIG. 8. The relaxation time $\tau(k)$, stretch exponent $\beta(k)$, and the Debye-Waller factor $A(k)$ extracted from the incoherent correlation functions, $F_s(k,t)$ and $F_s^Q(k,t)$, by fitting the long-time part of the respective correlation functions with a stretched exponential function.

another relaxation channel other than the α relaxation generated by the crossing-basin process. The existence of a short-time decay channel can also be seen from the presence of the initial rapidly increasing segment of the MSD curve of the quenched configurations. One of this short time decay channel could be the existence of the finer structures at the bottom of the potential basin. These finer structures have small surface roughness that cannot be felt by the system at that temperature. But when we quench the system, the resultant minimum location can be one of the basins belonging to these finer structures. Because these finer structures at the bottom of the basin have no constraining effect on the system motions, the system can move easily from one to another local minimum in these finer structures.

IV. CONCLUSIONS

We studied the dynamics of inherent structure by the process of quenching the original configuration generated by the MD simulation in the binary Lennard-Jones system near glass transition. We showed from the MSD and van Hove self-correlation function that the quenched configurations do not exhibit the cage effects that normally constrain the dynamics of original configurations at the intermediate time. We showed from the time correlation functions, both the self and coherent part, that the long-time relaxation remains the same in the quench process in all k values studied, but the short-time dynamics within the potential basin is nearly eliminated. We conclude that the collective, slow relaxation is due to crossing over different potential basins by the system phase point.

We acknowledge that our result, obtained from examination of collective motions of particles at different length scale (k values), is the same as the conclusion reached by Schroder *et al.* in Ref. [15] and by Sastry, Debenedetti, and Stillinger in Ref. [27]. They examined the self part of the correlation function of inherent structure at one k value and different temperatures, and found that the long-time α relaxation of the test particle is the result of the phase point of the system exploring different potential basins. We would like to note that, beyond the short-time region, motions of the test particle at high densities and very low temperatures are strongly coupled to the density fluctuation. Therefore, the long-time relaxation of the test particle is essentially dominated by the relaxation of the density fluctuation. It is then not surprising that our result obtained from examination of the k dependence of the density correlation function is similar to that obtained from calculating the test particle correlation function.

ACKNOWLEDGMENT

This research was supported by a grant from the Materials Chemistry Research Program of the U.S. DOE.

[1] E. Leutheusser, Phys. Rev. A **29**, 2765 (1984); U. Bengtzelius, W. Gotze, and A. Sjolander, J. Phys. C **17**, 5915 (1984).
[2] W. Gotze and L. Sjogren, Rep. Prog. Phys. **55**, 241 (1992).
[3] P. Gallo, F. Sciortino, P. Tartaglia, and S.-H. Chen, Phys. Rev. Lett. **76**, 2730 (1996); F. Sciortino, P. Gallo, P. Tartaglia, and S.-H. Chen, Phys. Rev. E **54**, 6331 (1996).
[4] M.D. Ediger, C.A. Angell, and Sidney R. Nagel, J. Phys. Chem. **100**, 13 200 (1996).
[5] C.Y. Liao, F. Sciortino, and S.H. Chen, Phys. Rev. E **60**, 6776 (1999).
[6] T. Gleim, W. Kob, and K. Binder, Phys. Rev. Lett. **81**, 4404 (1998).
[7] M. Goldstein, J. Phys. Chem. **51**, 3728 (1969).
[8] J.D. Bernal, Nature (London) **183**, 141 (1959).
[9] F.H. Stillinger and T.A. Weber, Phys. Rev. A **25**, 978 (1982); F.H. Stillinger, Science **267**, 1935 (1995).
[10] F. Sciortino, W. Kob, and P. Tartaglia, Phys. Rev. Lett. **83**, 3214 (1999).
[11] A. Scala, F.W. Starr, E. La Nave, F. Sciortino, and H.E. Stanley, Nature (London) **406**, 166 (2000).
[12] F.H. Stillinger and T.A. Weber, Phys. Rev. A **28**, 2408 (1983).
[13] S. Buchner and A. Heuer, Phys. Rev. Lett. **84**, 2168 (2000).
[14] T.B. Schroder and J.C. Dyre, J. Non-Cryst. Solids **235**, 331 (1998).
[15] T.B. Schroder, S. Sastry, J.C. Dyre, and S.C. Glotzer, J. Phys. Chem. **112**, 9834 (2000).
[16] W. Kob and H.C. Andersen, Phys. Rev. E **51**, 4626 (1995).
[17] M. Nauroth and W. Kob, Phys. Rev. E **55**, 657 (1997).
[18] S. Nose, Phys. Rev. E **47**, 164 (1993).
[19] W.H. Press, S.A. Teukolsky, W.T. Vetterling, and B.P. Flannery, *Numerical Recipes in C* (Cambridge University, Cambridge, England, 1992).
[20] J.P. Hansen and I.R. McDonald, *Theory of Simple Liquids* (Academic, London, 1986).
[21] J.P. Boon and S. Yip, *Molecular Hydrodynamics* (McGraw-Hill, New York, 1980).
[22] A. Rahman, Phys. Rev. **136**, A405 (1964).
[23] F. Sciortino, L. Fabbian, S.-H. Chen, and P. Tartaglia, Phys. Rev. E **56**, 5397 (1997).
[24] W. Gotze, in *Liquids, Freezing, and the Glass Transition*, edited by J.P. Hansen, D. Levesque, and J. Zinn-Justin (Elsevier Science, Amsterdam, 1991).
[25] F. Sciortino and P. Tartaglia, Phys. Rev. Lett. **78**, 2385 (1997).
[26] S.-H. Chen, C.Y. Liao, F. Sciortino, P. Gallo, and P. Tartagalia, Phys. Rev. E **59**, 6708 (1999).
[27] S. Sastry, P.G. Debenedetti, and F.H. Stillinger, Nature (London) **393**, 554 (1998).